Environmental Science and Pollution Research (2024) 31:57748–57764
https://doi.org/10.1007/s11356-024-34942-y

RESEARCH ARTICLE

Sorbent selection for the recovery of gallium and indium from aqueous solutions: a sustainable approach to the recovery of strategic metals from LED lamps

Patricia Sáez[1] · Eduardo Díez[1] · José María Gómez[1] · Carmen López[1] · Naby Conte[1] · Mercedes Lobete[1] · Araceli Rodríguez[1]

Received: 30 December 2023 / Accepted: 5 September 2024 / Published online: 18 September 2024

Abstract

Gallium and indium, metals present in light-emitting diode (LED) lighting technology, can be effectively recovered from aqueous solutions by sorption. For this purpose, carbonaceous materials, such as activated carbon, or low-cost biosorbents as beer bagasse, spent coffee grounds or peanut shells, and a low-cost zeolite as chabazite, were characterized by BET, FTIR, XRD, and SEM analysis prior use. Protonated chabazite, with high surface area (505 m^2/g) and a Si/Al molar ratio of 3.4, showed high sorption capacities for gallium (56 mg/g) and indium (92 mg/g), which is 10 to 30 times higher than those of our carbonaceous materials (T = 298 K, pH < 3, dosage = 1 g/L). Sorption experiments with both metals in solution showed a competitive effect between gallium and indium for the sorption sites of the chabazite, showing more affinity toward gallium than indium. $Ga^{3+}{}_{sorbed}/In^{3+}{}_{sorbed}$ molar ratio above 2 was achieved for the same initial concentration of both metals, increasing to almost 3 when the initial gallium concentration increased, which was appropriate since gallium concentration tends to be higher in LED chips. However, the sorption capacity for both metals was always around 0.35 mmol Ga + In/g. The selectivity of the chabazite was conditioned by different behavior of both metals in aqueous solution at the sorption pH (below 3.5) being the predominant species in solution $Ga(OH)^{2+}$ for gallium and In^{3+} for indium. Sorption with protonated chabazite can be used in the treatment of spent LEDs leachate for the dual purpose of water purification and selective metal separation.

Keywords Gallium · Indium · Sorption · Chabazite · Carbonaceous materials · LED recycling

Introduction

Aiming for the sustainable development of both economy and environment, a group of materials, known as "critical raw materials" (CRM), have gained importance in the European Union (European Commission, Directorate General for Internal Market, Industry, Entrepreneurship and SMEs 2023). The European Commission updates this list every 3 years since its creation in 2011 and, in accordance with the climate-neutrality target for 2050, the CRM list is expected to be one of the hottest topics in the years to come (Michaels 2021). These raw materials are gaining an increasing importance for the EU economy's growth, being crucial to reduce the existing dependence of materials from non-European countries and to ensure millions of European jobs over the next few decades (Nikulski et al. 2021). Some of those elements, in particular a certain group of metals known as "strategic metals," are prominent for their scarcity in the earth's crust, economic importance, risk of supply, and low or even non-existing recycling rates (Girtan et al. 2021). Gallium belong to that category, being crucial in the semiconductor manufacturing (Chen et al. 2018). Although indium has been recently removed from the strategic classification, the research on the extraction and recovery processes for both gallium and indium must be regarded to reduce the use of natural sources and for their applications (Khezerloo et al. 2023).

In relation to gallium, it is a high valuable metal whose main applications are focused on the semiconductor industry (Cenci et al. 2020). Concerning indium, is a soft silvery white

Responsible Editor: Ioannis A. Katsoyiannis

✉ Eduardo Díez
ediezalc@ucm.es

[1] Department of Chemical and Materials Engineering (CyPS Research Group), School of Chemical Sciences, Universidad Complutense de Madrid, 28040 Madrid, Spain

metal, which is mainly employed in the electronic industry for the manufacture of photoconductors or thermistors, and in the manufacturing of liquid crystal screens (Akcil et al. 2019). Both metals, Ga and In, are widely applied as semiconductors (as GaN, GaAs, or InGaN) in the manufacture of light-emitting diodes (LEDs) technology, which includes many types of displays and screens (Khezerloo et al. 2023) and lighting sources (Chen et al. 2020). LED lighting technology has established itself as an alternative to traditional bulbs, fluorescent, and incandescent (Zamprogno Rebello et al. 2020), standing out for its lower usage cost due to longer lifetimes (25,000 h as compared with 12,000 h for fluorescent lamps and 1000 h for incandescent bulbs (Richter et al. 2019)) and higher luminous effectiveness (Martins et al. 2020). LED lighting technology had a penetration rate of 47% in the global lighting market in 2019, but some studies forecast that the 100% of market share will be reached in 2030 (Nikulski et al. 2021), just for being a more sustainable and environmentally friendly alternative. It is not only being used for household applications, but also for street lighting and industry applications (i.e., automotive industry) (Balinski et al. 2022). In addition, gallium and indium are important elements for the manufacture of copper-indium-gallium-selenide (CIGS) thin-film photovoltaic solar cells. Therefore, demand for gallium and indium is likely to increase by as much as 2.5 times between 2030 and 2050 compared to current levels (Directorate-General for Internal Market et al. 2020).

However, it is mandatory to recognize the problem associated with the increasing consumption of LED lamps. The generation of waste from electrical and electronic equipment (WEEE), also known as e-waste, is a notable problem linked to the increased consumption of electrical devices (de Oliveira et al. 2021). LED lamps waste is no exception. Globally, more than 62 Mt of e-waste were generated globally, with less than one quarter being collected and recycled (Balde 2024). It is estimated that over 74.7 Mt will be generated by 2030, with an annual growth rate of 2% (Ahirwar and Tripathi 2021). Luminaire waste, including LED bulbs, accounted for approximately 3% of that waste generation in 2022, with only a minimal fraction of 5% being recycled (Balde 2024). This e-waste generation is not accompanied by a proper recycling, which is crucial to meet the 12th Sustainable Development Goal (*Responsible consumption and production*) (Rahimifard and Trollman 2018). In 2022, the UN Global E-waste monitor revealed that world's generation of e-waste is rising five times faster than documented e-waste recycling, with only a 22.3% of e-waste being properly collected and recycled (Kuehr 2024). This fraction is insufficient to overcome another problem: the increasing scarcity of raw materials for manufacturing these luminaire devices. Metals such as gallium and indium have a negligible recycling rate (less than 1% for gallium and 0% for indium) (European Commission. Directorate General for Internal Market, Industry, Entrepreneurship and SMEs 2023). China, responsible for 94% of global market share of gallium and 50% of indium (European Commission. Directorate General for Internal Market, Industry, Entrepreneurship and SMEs. 2023), is curbing the exports of metals such as gallium and indium, since August 1st, 2023, in order to strengthen their own economy (Reuters 2023). Therefore, studying the feasibility of recycling those LED lamps and the metals contained in the LED module opens a unique door for the concept of circular economy, with these wasted chips being a new source of secondary raw material for the manufacture of a new generation of lighting systems. Otherwise, the increasing disposal and accumulation of WEEE will affect the environment (air, soil, and specially water), causing hazardous effects to humans and other living beings and organisms (Rautela et al. 2021).

In recent years, among the alternatives for obtaining indium and gallium, their recovery from wastewater leachates and luminaire wastes is gaining attention mainly because it involves a double objective: purifying water on the one hand, and recovering the important raw materials on the other hand, within the framework of a circular economy and considering the Sustainable Development Goals. Among the different sources of wastewater, those coming from electronics industry are especially suitable for the recovery of gallium and indium, as they usually contain both metals simultaneously. Therefore, efforts should focus on developing a suitable technique to selectively separate these two ions from the same aqueous matrix.

Several alternatives have been studied in the literature, when dealing with metal-contaminated wastewater. Filtration (Lahti et al. 2020), chemical precipitation (Qasem et al. 2021), membrane processes (Lahti et al. 2020), solvent extraction (Liu et al. 2006; Song et al. 2020; Drzazga et al. 2021), or electrochemical methods (Grevtsov et al. 2021) are available options. However, these processes have significant drawbacks, such as sludge production, large operation costs, or incapability of reaching a complete removal. Adsorption has emerged as a promising technology, especially suitable when a high selectivity for a specific metal (as is the case of this study) or the pre-concentration of trace metal amounts is required.

The adsorbents used for adsorption are very varied, including zeolites, activated carbon, minerals, oxides, and many others. The adsorbent is a crucial part for the feasibility of the operation: its cost will determine the profitability of the process, and their selectivity toward the selected adsorbate will become key to avoid further purification processes (Saravanan et al. 2021; Shrestha et al. 2021). Recent efforts have concentrated on finding relatively inexpensive and available adsorbents. Low-cost sorbents such as industrial and agricultural wastes and by-products (sawdust, straws, fly ash, mud, oil, bagasse,

shells) and natural materials stand out for being relatively cheap, as they are highly and naturally accessible (Worch 2012). Among natural materials, one especially adequate is a natural zeolite, chabazite.

Chabazite is a natural zeolite member of chabazite group that can be found in the cavities of basaltic rocks all around the world. Its generic chemical formula is $(Ca_{0,5},Na,K)_4[Al_4Si_8O_{24}]\cdot 12H_2O$, with a silicon to aluminum ratio ranging from 2 to 5, what confers thermal stability to the zeolite. The crystal structure of chabazite consists of a three-dimensional pore structure with an opening of 3.8 Å, occupied by water and exchangeable cations, such as Na^+ or K^+. These characteristics make chabazite a suitable adsorbent for metal ions removal from wastewater.

Previous studies have employed chabazite as an adsorbent for different compounds, which gives an idea of its potential applicability. Aysan et al. (2016) and Solisio and Aliakbarian (2017) employed this natural zeolite to successfully remove methylene blue from aqueous solutions. It has also been employed to separate different compounds from gas streams, such as N_2, O_2, and Ar (Singh and Webley 2005) or N_2, CO_2, and CH_4 (Watson et al. 2012). Other applications of this solid as adsorbent have been CO_2 capture (Zhang et al. 2008; Pham et al. 2014), separation of CO_2/CH_4 mixtures (Shang et al. 2020), or alkane adsorption (Denayer et al. 2008; Göltl and Hafner 2011).

Despite its suitable characteristics, chabazite has not been deeply studied in literature as potential adsorbent for metal removal. Some references can be found in literature; however, none of them directly was applied to recover gallium and indium. Some authors (Gallant et al. 2009) compared chabazite and clinoptilolite as adsorbents to recover Cs, Co, Sr, Cu, Cd, and Zn, found in effluents of nuclear operations. They concluded that the better adsorption capacity of chabazite could be attributed to its larger pore volume as well as its high silicon to aluminum ratio. Other studies (Egashira et al. 2012) employed chabazite, mordenite, and clinoptilolite, to adsorb Cu, Zn, and Mn. They also concluded that the cation exchange capacity of natural zeolite increases with increasing aluminum content. Some other authors (Yakout and Borai 2014) employed chabazite to remove Cd from aqueous solutions, obtaining a maximum cadmium adsorption capacity of 120 mg/g, and concluding that the adsorption process is strongly pH dependent in the 2.5–8.5 range. Additionally, other references (Ibrahim et al. 2016) employed phillipsite–chabazite tuffs to adsorb Mo and Ni from aqueous solutions, reaching a Mo removal efficiency of 76% and a Ni removal efficiency above 90%. Finally, more recent investigations (Pinedo-Torres et al. 2023) applied a protonated chabazite to adsorb metals such as As(V), Pb(II), Cd(II), and Cr(III) cations from aqueous solutions, reaching capacities higher than 100 mg/g for Pb^{2+} ions, highlighting the great potential of this natural zeolite to adsorb metallic cations.

Currently, most of the world's gallium supply comes from bauxite mining and sediment-hosted lead–zinc (Pb–Zn) resources, with an average content of Ga in bauxite about 50 mg/kg (Qi et al. 2023). The main source of indium is zinc concentrates (indium containing 0.0001–0.1%), recovered as a byproduct in the smelting of zinc ore and tin smelting process. However, the LED module, according to our measurements, contains about 1100 mg/kg of gallium and above 400 mg/kg of indium. Other sources indicate that the Ga content in LEDs is around 0.25–4 wt% (Balinski et al. 2022). This is a much higher gallium content than in bauxite, demonstrating the importance of LED waste as secondary sources of these metals. Pretreatment stages for metal recovery usually comprises physical processes such as crushing, classification, electrostatic and magnetic separation, plus calcination if needed (Mir et al. 2022; Zheng et al. 2024). Despite this stage of the whole process being energy intensive, it is important to consider that gallium production from bauxite and zinc ores (Bayer process) also involves similar stages of physical treatment (crushing, milling, etc.) and high temperature reactions to obtain the red mud or the leach liquors where metal concentration of gallium is quite low compared to those concentrations found in LED wastes (Zhao et al. 2012; Lu et al. 2017). Therefore, we consider our approach to recover gallium from LED waste (and sorption as the final extraction stage of the process) being worth investigating.

Therefore, the main aim of this work is to study the selective recovery gallium and indium, present in leachate of spent LED, from aqueous solutions, simulating concentrations comparable to those found in leachates, by sorption onto a low-cost zeolite, chabazite, barely studied in the literature. As explained, the rising importance of metals such as gallium and indium, both crucial for semiconductors manufacture, guide our efforts for their recovery, over other metals present in the spent LED chips. To adsorb ions such as Ga^{3+} and In^{3+}, materials such as activated carbons (Alguacil et al. 2016), biosorbents (Pennesi et al. 2019), nanofibers (Segala et al. 2023), and zeolites (Ujaczki et al. 2019) have been employed; nevertheless, the use of natural and low-cost zeolites remains to be explored. This work provides a comparison between chabazite, carbonaceous materials such as mesoporous carbon, bagasse, coffee grounds, and other low-cost biosorbents, in which chabazite has emerged as the most effective option, and those sorbents found in literature. The removal of both metals primarily and the possibility of removing one of them separately was studied in depth. A complete characterization of the chabazite was carried out, for a better understanding of the adsorption mechanism. Due to the nature of some of the sorbents used, the removal of cations from aqueous solution was expected to occur by both

adsorption and ion exchange. Therefore, the term sorption was used since adsorption and ion exchange are sorption processes (Haan 2015).

Experimental

Chemicals

Gallium (III) and indium (III) nitrate hydrate ($Ga(NO_3)_3 \geq 99.9\%$, $M_w = 255.74$ g/mol and $In(NO_3)_3 \geq 99.9\%$, $M_w = 300.83$ g/mol) were provided by Sigma-Aldrich. Hydrochloric acid ($HCl \geq 37\%$, $M_w = 36.46$ g/mol) was supplied by Fluka. Silica gel (SiO_2, pore size 150 Å, particle size 75–250 µm, $M_w = 60.08$ g/mol) supplied by ACROS Organics, sucrose ($C_{12}H_{22}O_{11}$, ≥ 99.5%, $M_w = 342.3$ g/mol), hydrofluoric acid (HF, 40%, $M_w = 20.01$ g/mol), supplied by Sigma-Aldrich, ethanol (C_2H_6O, 96%, $M_w = 46.07$ g/mol) and sulfuric acid (H_2SO_4, 98%, $M_w = 98.08$ g/mol) from Panreac, were all employed for the mesoporous activated carbon synthesis. Ultrapure water was used to prepare the solutions.

Sorbents

Several sorbents were employed in this study, such as beer bagasse (BB), spent coffee grounds (SCG), peanut shells (PS), mesoporous activated carbon (MAC), and chabazite (CHA), a low-cost zeolite. Beer bagasse was supplied by the company Cherry Below Brewery, SL (Segovia, Spain). The bagasse was pre-carbonized at 100 °C for 6 h and then at 150 °C for another 6 h. It was then ground, sieved (< 500 µm), and dried. Spent coffee grounds and peanut shells were washed and dried before use. Mesoporous carbon was synthesized following the replica method, according to previous works of the research group (Galán et al. 2013). Chabazite was supplied by St. Cloud Mining (New Mexico, EEUU) and its main constituent was chabazite with clinoptilolite, quartz, feldspars among other impurities, according to the supplier. Regarding to chemical composition of zeolite sample, the analysis carried out by the distributor revealed that the dominant cation was sodium. The chemical composition as well as other properties of the zeolite supplied are summarized in Table 1.

Before used as sorbent, the chabazite was washed with deionized water to remove its turbidity, dried at 373 K for 24 h, and sieved to obtain a 1.00–1.18 mm size fraction. Furthermore, to improve its sorption capacity and to ensure an acid medium to avoid Ga^{3+} and In^{3+} ions precipitation, the chabazite was further treated with HCl to obtain the protonated form (H-CHA). The concentration of acid solution selected was 0.05 M to ensure a partial protonation without dealumination. The protonation was carried out by disposing the zeolite on a filter and adding the 0.05 M HCl solution, keeping a ratio of 50 mL/g of zeolite. This technique was previously used by the research group to protonate other zeolites (Sáez et al. 2021). After protonation, the zeolite was rinsed and washed until no chlorides were found and dried at 373 K for 24 h. Finally, the treated zeolite was characterized and compared with raw chabazite to detect any possible structural alteration as well as to analyze the modification applied.

Table 1 Properties of chabazite based on supplier analysis

Parameter	Value
Chemical composition (%)	SiO_2 68.1; Al_2O_3 18.59; Fe_2O_3 2.84; CaO 0.27; MgO 0.75; Na_2O 8.32; K_2O 1.12
Density (g/cm^3)	1.73
Pore size (Å)	4.1–3.7
Cavity size (Å)	11.0–6.6
Surface area (m^2/g)	520
Pore volume (cm^2/g)	0.468
Mohs' hardness scale	4–5
Stability	pH of 3 through 12
Ion exchange capacity (meq/g)	2.50

Characterization

Different characterization techniques were used to study the different properties of the sorbent materials. X-ray diffraction (XRD) patterns with CuKα1 radiation for 2θ between 5° and 50° scanning range and a step size of 0.1 were recorded on a SIEMENS-D501 diffractometer. Chemical composition of chabazite was determined using X-ray fluorescence (XRF) in an Aχios instrument. The degree of protonation was calculated from the XRF results according to Eq. 1.

$$\%H^+ = \left(\frac{Al - \text{Cations}}{Al}\right) \bullet 100 \quad (1)$$

where *Al* is the aluminium content and *Cations* is the sum of the sodium, calcium, and potassium content, all in molar units. In zeolites, the aluminium content determines the ion exchange capacity. For each aluminium, a negative charge is produced in the structure, which must be compensated by cations such as sodium or protons to maintain the electrical neutrality of the framework. Since XRF analysis does not detect protons, the difference between aluminium and detected cations was assigned to H^+.

Adsorption–desorption isotherms of N_2 at 77 K were obtained using a MICROMERITICS ASAP 2020 apparatus. Zeolites were degassed at 573 K for 3 h, while organic sorbents were degassed at 523 K. Total specific surface area and volume of pores were determined using the

Brunauer–Emmett–Teller (BET) equation and the single-point method ($p/p_0 = 0.99$), while the pore size distribution (PSD) curves were calculated from the desorption branch by the Barret-Joyner-Halends (BJH) method. Micropore volume was calculated using the *t*-plot method. Fourier transform infrared spectroscopy (FTIR) analysis was applied to analyze the surface chemistry of the sorbents, using a Nicolet iS50 FTIR spectrophotometer in the infrared spectrum (400–4000 cm^{-1}). The analyses were carried out by the Center for Spectroscopy and Correlation of Complutense University of Madrid. SEM analyses were conducted by using a scanning electron microscope JSM 6400 (JEOL), by the Spanish National Center for Electron Microscopy (ITCS). For further study of chemical speciation of gallium and indium, the Medusa-Hydra Chemical Equilibrium Diagrams™ software (developed by the Department of Chemistry of Kungliga Tekniska ögskolan (KTH) Royal Institute of Technology) has been employed.

Sorption experiments

Sorption experiments were carried out at constant temperature of 298 K and agitation rate (approximately 250 rpm). pH was kept below 3.5 to avoid the precipitation of metal ions. Different metal concentrations and sorbent doses were employed to select the best sorbent. After adsorption, the liquid phase was separated from the solid phase by filtration with a 0.2 µm filter.

Two kinds of experiments were made: (i) equilibrium sorption experiments with a single metal in solution, to obtain the maximum adsorption capacity for each metal and sorbent, and (ii) competitive sorption experiments with both metals in solution (Ga^{3+} and In^{3+}) with the best sorbent to establish the affinity for each of them. Regarding the competitive kinetics experiments, different ratios of [Ga]/[In] were employed (from 0.5 to 2). In this case, samples were initially taken every 15 min until the first 90 min, after which they were taken every 60 min.

The metal ion concentration remaining in solution was determined by atomic absorption spectroscopy (Shimadzu AA-7000). The amount of metal ions removed by chabazite was calculated using the Eqs. 2 and 3.

$$q\left(\frac{\text{mg}}{\text{g}}\right) = \frac{\left(C_0 - C_t\right) \cdot V}{m} \tag{2}$$

$$\text{Removal}\ (\%) = \frac{\left(C_0 - C_t\right)}{C_0} \tag{3}$$

where q is the amount of metal adsorbed per gram or adsorption capacity (mg/g), C_0 is the initial metal ion concentration (mg/L), C_t is the metal ion concentration after time t (mg/L), V is the solution volume (L), and m is the mass of the sorbent (g).

Result and discussion

Characterization

Figure 1 displays the XRD patterns of zeolites (CHA and H-CHA). The results revealed that the chabazite employed showed the characteristic peaks of chabazite (*) with some impurities (•), already indicated in the supplier's data sheet (Aysan et al. 2016). After the treatment with HCl 0.05 M (H-CHA), the zeolite retained the crystalline structure showing the same peaks as chabazite indicative of the CHA framework. The slight decrease in the peak intensity was due to the ion-exchange of Na^+ by H^+ (Kennedy and Tezel 2018). Therefore, the acid treatment with low concentrated hydrochloric acid did not modify the CHA framework of the chabazite used.

Figure 2 displays the FTIR spectra of carbonaceous (Fig. 2(A)) and zeolitic materials (Fig. 2(B)). The absorption band at approximately 3400–3300 cm^{-1} was assigned to the O–H stretching bonded and non-bonded hydroxyl groups. Beer bagasse and spent coffee grounds showed similar absorption bands at 2900 and 2850 cm^{-1} corresponding to C-H stretching and vibrational deformation from aliphatic alkanes (Anukam et al. 2016). In carbonaceous sorbents, the peaks at 1750–1600 cm^{-1} were due to the carboxyl groups of carboxylic acid or its ester (Kim and Kim 2020). The band at approximately 1400 cm^{-1} was associated with the presence of aliphatic bonds ($-CH_2$, $-CH_3$) that form the basic structure of lignocellulosic materials. Finally, the peak around 1100 cm^{-1} was due to

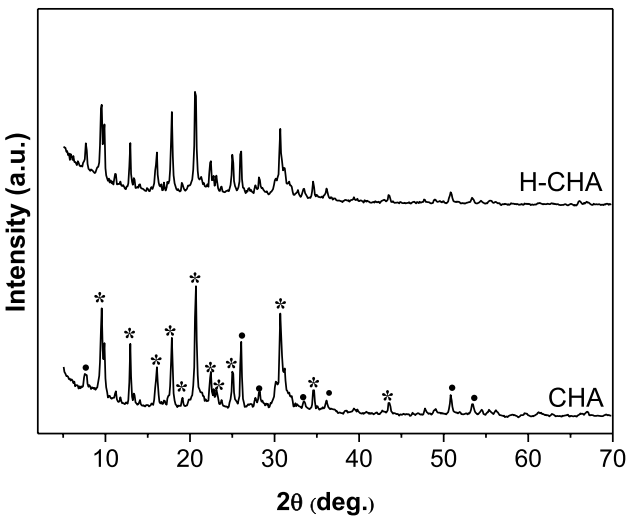

Fig. 1 XRD pattern of CHA and H-CHA

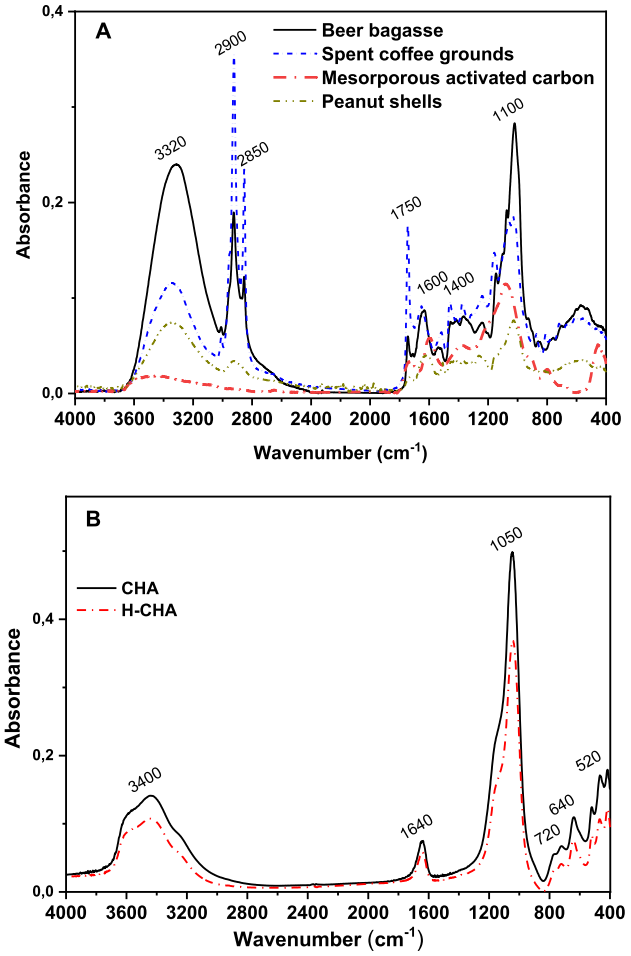

Fig. 2 FTIR spectra of carbonaceous (**A**) and zeolitic (**B**) sorbents

the stretching vibration of the C–OH bond of alcohols or phenolic groups.

In relation to the chabazite, the FTIR spectrum (Fig. 2(B)) is composed by two groups of vibrational frequencies: internal vibration of T-O (T = Si and Al) and vibration of external bonds between tetrahedrons, whose peaks appear at wavenumbers ranging from 1200 to 400 cm^{-1}, and the bands or peaks assigned to the presence of structural water (from 1600 to 3700 cm^{-1}). More precisely, in the CHA spectrum, the zeolite showed strong bands between 520 cm^{-1} and 640 cm^{-1} which correspond to 6-membered rings structural units. The band observed at 720 cm^{-1} indicated 4-membered ring structure. Finally, the band at 1050 cm^{-1} indicated T-O stretching vibration. These structural bands were also present in the H-CHA spectra, confirming that the acid treatment did not modify the CHA framework, such as the XRD analysis concluded. Concerning the other peaks identified in the spectra (3400 cm^{-1} and 1640 cm^{-1}), they corresponded to isolated O–H stretching and H_2O bending respectively (Mozgawa et al. 2011).

XRF analysis of unmodified chabazite showed a silicon/aluminum molar ratio of 3.2 with sodium as the majority cation (3.4% molar) and calcium and potassium as the other compensation cations (molar percentages around 0.5% and 0.7% respectively). After acid treatment, the Si/Al molar ratio increased slightly to 3.4, so that the dealumination of the zeolite was discarded. The protonation degree of the chabazite (Eq. 1) was increased from 27% for CHA to 44% for H-CHA after the washing with HCl 0.05 M. Therefore, modification of the zeolite using diluted acid increased the number of protons while maintaining the crystalline structure and the crystallinity degree.

The nitrogen adsorption–desorption isotherms of CHA, H-CHA and activated mesoporous carbon are shown in Fig. 3. Table 2 shows the textural properties of the sorbents.

As seen in Fig. 3, the adsorption–desorption isotherms of CHA and H-CHA exhibited the typical shape of the microporous materials, without significant changes between them. The isotherms belong to type I in the IUPAC classification with H4 hysteresis loop, attributed to microporous materials, with a large amount adsorbed until 0.2 p/p_0 followed by a plateau till 0.8–0.9 p/p_0 and finally, a sharp increase due to the macropores associated to the intraparticular cavities. On the other hand, mesoporous activated carbon showed an isotherm shape that belongs to type IV,

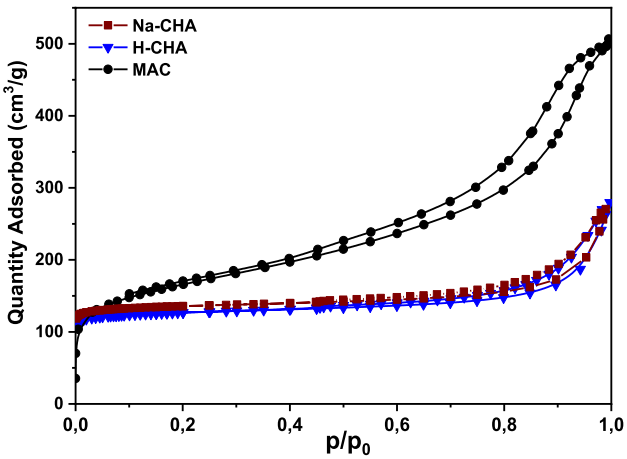

Fig. 3 N_2 adsorption–desorption isotherms for natural and modified chabazite (CHA, H-CHA) and mesoporous activated carbon (MAC)

Table 2 Textural properties for CHA and H-CHA

Sample	Surface area BET (m^2/g)	Micropore area (m^2/g)	Micropore volume (cm^3/g)	Total pore volume (cm^3/g)
CHA	544	479	0.18	0.34
H-CHA	505	434	0.16	0.39
MAC	350	60	0.03	0.92

typical of mesoporous materials, with a hysteresis loop associated with capillary condensation in the mesopores. As observed in Table 2, the acid treatment produced in the chabazite caused a slight decrease in the BET surface area as well as in the amount of micropores. However, for MAC the main contribution to the specific surface area and pore volume was due to mesopores. In beer bagasse (BB), spent coffee grounds (SCG), and peanut shells (PS), the specific surface area was very low (< 5 m^2/g), almost negligible, being external surface the majority of the inner structure.

Lastly, scanning electron microscopy (SEM) images of CHA and H-CHA samples are displayed in Fig. 4.

As displayed in Fig. 4, chabazite zeolite type is composed of different aggregates as well as cube or rhombohedral crystals (CHA × 5000) typical of sedimentary chabazite and plate-shaped crystals corresponding to clinoptilolite impurities (Mumpton and Ormsby 1976). Acid treatment did smooth the surface appearance. This effect was observed with clinoptilolite-type zeolite by other authors who related it to the exchange of cations for protons (Korkuna et al. 2006). In addition, the size of the chabazite crystals seems decreased as can be observed in Fig. 4 since at 5000 × magnification for CHA the crystals are clearly visible, whereas for H-CHA no (yellow circle in Fig. 4).

Batch sorption results

Batch experiments were carried out to select the best sorbent to study the bimetallic adsorption. Figure 5 displays the adsorption capacities of the studied sorbents. Carbonaceous sorbents showed lower capacities (< 3 mg/g) for both metals compared to zeolites (> 20 mg/g). Among the carbonaceous sorbents, MAC and BB showed higher adsorption capacities (≈ 3 mg/g) for both In and Ga than SGC and PS (≈ 2 mg/g). However, the adsorption capacity of the chabazites was clearly upper than the other sorbents, reaching 65 mg/g of In and 45 mg/g of Ga for the H-CHA zeolite. Therefore,

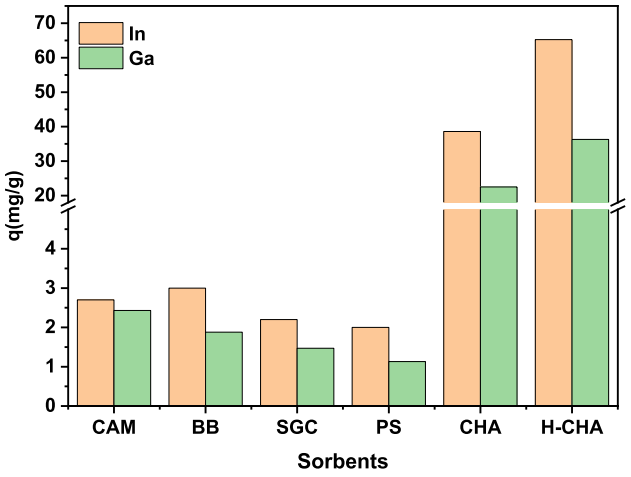

Fig. 5 Adsorption of Ga and In on the studied sorbents. Carbonaceous sorbents (CAM, BB, SGC and PS): [Ga] = [In] = 20 ppm, sorbent dose = 5 g/L, time = 24 h, T = 25 °C, pH < 3.5. Zeolites (CHA and H-CHA): $[Ga^{3+}] = [In^{3+}] = 40$ ppm, sorbent dose = 1 g/L for CHA and 0.5 g/L for H-CHA, time = 3 days, T = 25 °C, pH < 3.5

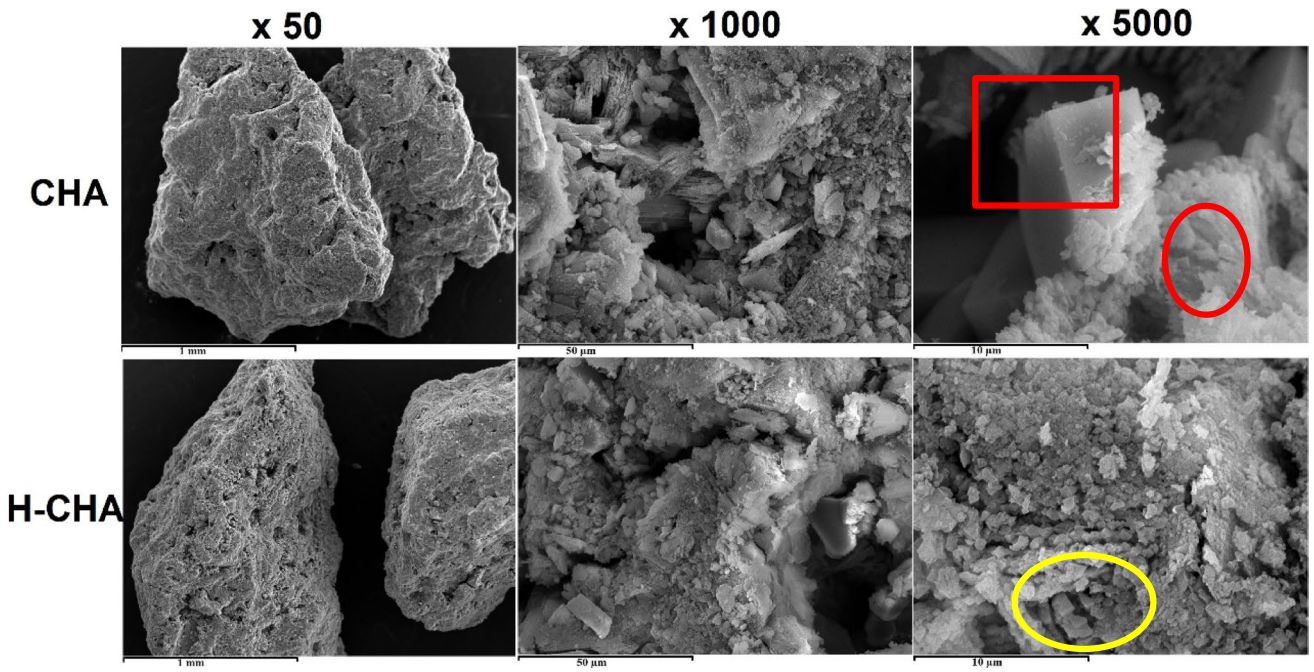

Fig. 4 SEM images of CHA and H-CHA at different magnifications

there was a huge difference between these two types of sorbents for the sorption of Ga and In. The ion exchange capacity of the zeolite was the main factor for the sorption of these metal cations, with protonation being necessary to work below pH 3.5, avoiding the precipitation of these metals. For the carbonaceous materials, the sorption process is driven by mechanisms such as ion exchange between H^+ ions present in oxygenated groups and the cations in the solution, metal complexation, and adsorption onto aromatic rings due to π-cation interactions (Conte et al. 2022). However, it is nowhere near the sorption potential that the natural zeolite has shown. BET surface area (Table 2) of chabazites is 45–55% higher than those of mesoporous carbon, and way higher than other biosorbents such as beer bagasse or peanut shells, with little to no porosity. Chabazite also presents greater cation exchange capacity, due to its inherent characteristics provided by its structure (Abdelwahab and Thabet 2023). Chabazite structure is formed by *d6r* hexagonal prism and *cha* blocks joined by six member rings (Fig. 6). There are four cationic sites: site I (hexagonal prism) in the centre of a double six-ring prism, site II (supercage) on the axis of the six prism triad, but shifted into the supercavity, site III in the supercavity, and near the four ring window and site IV near the eight ring opening (González-Crisostomo et al. 2022). CHA framework has a pore size of 3.80 × 3.80 Å, variable due to considerable flexibility of framework, e.g., for Al-CHA it varies at 3.84 × 3.89 Å or for Si-CHA at 3.80 × 3.90 Å (Baerlocher et al. 2007; Yue et al. 2022). In any case, the ionic diameter of gallium (1.24 Å) and indium (1.62 Å) is smaller than the pore size of chabazite (3.8 Å), being able to access the supercavity (diameter 7.37 Å) with no steric hindrance, occupying positions in sites II, III, and IV (Foster et al. 2006, 2007). The presence of exchangeable cations in this type of chabazite (mainly Na^+, but also Ca^{2+}, K^+) makes it ideal for the uptake of cationic species such as $Ga(OH)^{2+}$ and In^{3+}, to balance the negative charge of the structure originated by the trivalent aluminum ions (Breck 1973). Carbonaceous materials, despite having good potential for ion-exchange and metal complexation, because of the carboxylic acid functional groups found in those carbon structures (see FTIR analysis, Fig. 2) seem to have weaker cationic exchange potential (El Ouardi et al. 2023). For all the above reasons, H-CHA was selected for further study of gallium and indium sorption.

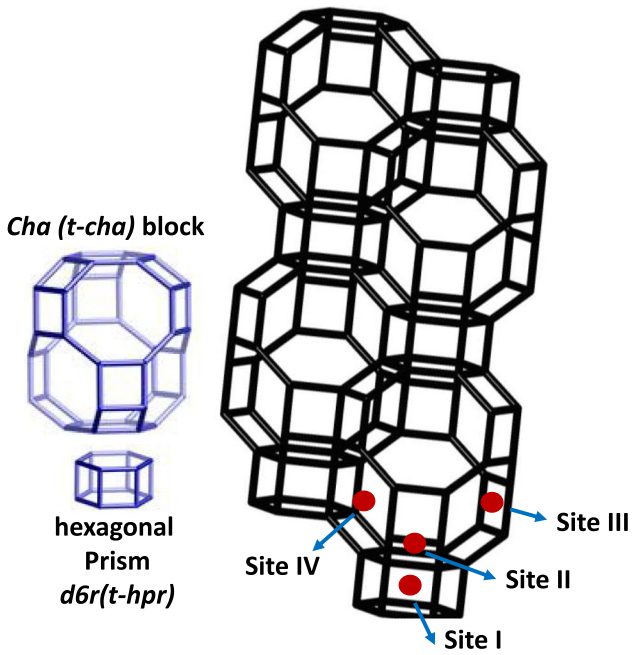

Fig. 6 Framework of chabazite viewed normal [001]

Equilibrium adsorption

Gallium and indium sorption equilibrium isotherms at 298 K were carried out on H-CHA zeolite to understand the sorption mechanism. The equilibrium experiments were carried out by increasing the initial concentration of the metal ion from 10 to 200 mg/L. The pH was kept stable at a value of around 2.8. The results are shown in Fig. 7.

Regarding the type of adsorption isotherm, according to Giles classification (Giles et al. 1960), they can be classified as H2 for gallium adsorption isotherm and H4 for indium adsorption isotherm. The isotherm group H refers to a high affinity between adsorbate and adsorbent. As for the subgroup, type 2 for gallium presented a plateau indicated that the sorbent surface area was completed, and the surface area was saturated. On the other hand, subgroup type 4 for indium indicated that H-CHA zeolite can develop new sorption sites, or reorient the position of the adsorbed indium, allowing the sorption of more

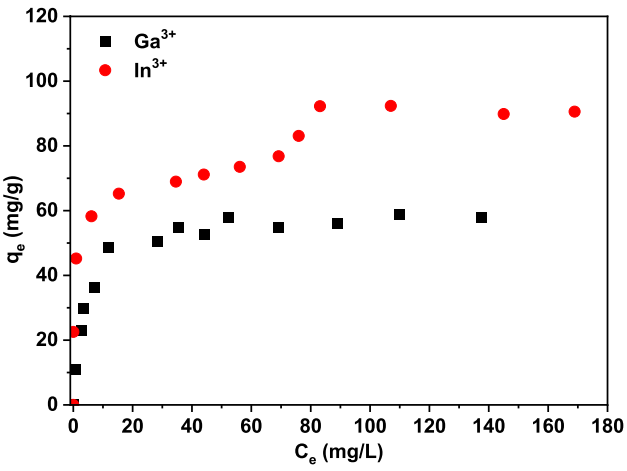

Fig. 7 Gallium and indium sorption isotherms at 298 K on H-CHA with sorbent doses of 1 g/L at free pH (< 3.0) and equilibrium time = 3 days

indium cations. This difference was due to the behavior of both metals in aqueous solution with pH. Figure 8 displays the speciation diagrams of both metals carried out with Medusa software. This software allows to develop a chemical diagram of metal speciation in terms of pH, metal concentration, and ionic species that can appear in the solution. As it can be observed in Fig. 8 at pH 3, for gallium, the predominant specie were the soluble complexes $Ga(OH)^{2+}$, which can occupy ion-exchange sites (Phadke et al. 2018). However, in the case of indium, the main species were the In^{3+} cations. Although both species have access to the ion exchange sites located within the supercavity (diameter 7.37 Å) accessible through the 3.8 Å channels, their different ionic radii lead to a different realignment of the cations (Rivera-Ramos and Hernández-Maldonado 2007).

The adsorption capacities were significant for both metals, reaching 92 mg/g for In^{3+} and 56 mg/g for Ga^{3+}, being 1.6 times higher for In^{3+} ($q_{In}/q_{Ga} = 1.6$). However, to make a better comparison between the two metals, the adsorption capacities should be expressed in mmol/g, as there is a large difference between their atomic weights (Mw_{Ga}: 69.7 and Mw_{In}: 114.8, $Mw_{In}/Mw_{Ga} = 1.6$). Then, the adsorption capacities were similar with 0.79 mmol/g for In^{3+} and 0.83 mmol/g for Ga^{3+} ($q_{In}/q_{Ga} = 0.95$). Therefore, all other results will be expressed in this way.

To give some context and put into perspective our results, Tables 3 and 4 overview the advantages of using low-cost

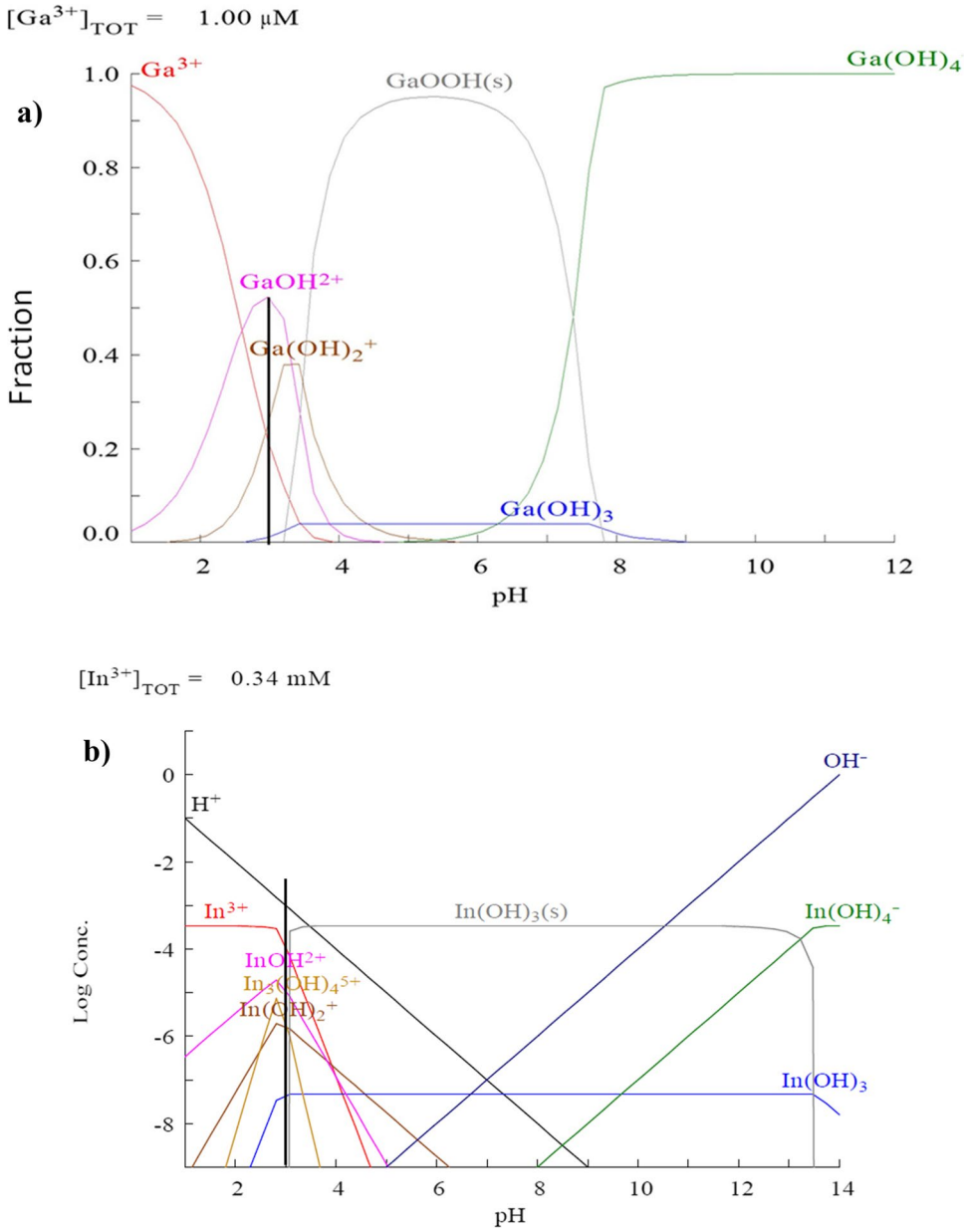

Fig. 8 Speciation diagrams for gallium (a) and indium (b)

Table 3 Adsorption removal capacities of gallium on different adsorbents

Adsorbent	$[Ga^{3+}]_0$ (mg/L)	q_{max} (mg/g)	pH	Temperature (°C)	Reference
8-hydroxyquinoline and 8-hydroxyquinaldine on chitosan-silica	100–300	27	12.25	20	Roosen et al. (2017)
Biogenic elemental tellurium nanoparticles	10	74	2.8	25	Saikia et al. (2022)
Polyacrylonitrile nanofibers-D2EHPA	20	33.1	2.5	45	Segala et al. (2023)
Mesoporous activated carbon	45	6.5	Below 3.2	25	Sáez et al. (2023)
Protonated clinoptilolite	45	4.9	Below 3.2	25	Sáez et al. (2023)
P507-TBP/SiO_2–P	25	59.9	3.3	25	Meng et al. (2021)
HY zeolite	50	7.9	5	20	Ujaczki et al. (2019)
Amidoxime resin	190	29.2	N/A	25	Zhao et al. (2016)
$CoFe_2O_4$-zeolite	0.08	87	5	25	(Zhao et al. 2015)
Chabazite	40	56	Below 3.5	25	This work

Table 4 Adsorption removal capacities of indium on different adsorbents

Adsorbent	$[In^{3+}]_0$ (mg/L)	q (mg/g)	pH	Temperature (°C)	Reference
Lewatit® TP207	100	55	3.4	25	Lee and Lee (2016)
Ascophyllum nodosum brown alga	200	63	3	25	Pennesi et al. (2019)
Phosphorylated sawdust	20	1.1	3.5	25	Jeon et al. (2015)
Mesoporous activated carbon	60	9.0	3.5	25	Díez et al. (2020)
D2HEPA-SiO_2-Polymer	8000	41.4	1	25–45	Qin et al. (2023)
Carbon nanotubes	10	40	10	60	Alguacil et al. (2016)
$CoFe_2O_4$-zeolite	0.08	94.8	5	25	Zhao et al. (2015)
UiO-66	21.3	11.8	3	25	Zeng et al. (2022)
Nano-TiO_2	15–60	6.5	3.5–4	25	Zhang et al. (2009)
Chabazite	40	92	Below 3.5	25	This work

Table 5 Isotherm models applied the equilibrium sorption of Ga^{3+} and In^{3+} onto H-chabazite

Isotherm model	Equation	Isotherm type
Langmuir (Langmuir 1917)	$q_e = \frac{q_{sat} \cdot b_L \cdot C_e}{1+b_L \cdot C_e}$ (4) $R_L = \frac{1}{1+b_L \bullet C_0}$ (5)	H2; L2
Freundlich (Freundlich 1906)	$q_e = K_F \cdot C_e^{1/n_F}$ (6)	H2; H4
Sips (Sips 1950)	$q_e = \frac{q_{sat} \cdot (b_S \cdot C_e)^{1/n_S}}{1+(b_S \cdot C_e)^{1/n_S}}$ (7)	H2; L2
Double Langmuir (Gómez et al. 2012)	$q_e = \frac{q_{s1} \cdot k_1 \cdot C_e}{1+k_1 \cdot C_e} + \frac{q_{s2} \cdot k_2 \cdot C_e}{1+k_2 \cdot C_e}$ (8) $k_2 = \alpha \cdot C_e^{\beta}$ (9)	H4; L4

chabazite in terms of gallium and indium capacity sorption, compared to other microporous or mesoporous adsorbent materials found in literature. It can be found how among the adsorbents found in literature, only cobalt ferrite-coated zeolite and nanoparticles of tellurium can match the adsorption results of the zeolite employed in our work, without considering the natural and low-cost origin of our adsorbent.

To describe the equilibrium sorption of Ga^{3+} and In^{3+} on H-CHA, several theoretical isotherms model have been selected, taking in consideration the type of isotherm (Hinz 2001). For Ga^{3+} isotherm, the employed models were Langmuir (Eq. 4), Freundlich (Eq. 6), and Sips (Eq. 7), whereas for In^{3+} isotherm were Langmuir (Eq. 4), Freundlich (Eq. 6), and Double Langmuir (Eqs. 8 and 9). The isotherm model equations are summarized in Table 5. For Langmuir model application, the constant separation factor or equilibrium parameter was calculated (Eq. 5), to determine the favorability or unfavourability of adsorption (Hall et al. 1966).

Where b_L is a constant describing the affinity between the adsorbent and adsorbate (L/mmol); q_{sat} is the maximum sorption capacity onto the monolayer (mmol/g); R_L is the constant separation factor, evaluating the favorability of the adsorption isotherm in terms of its shape: when $R_L > 1$ the adsorption is unfavorable, $R_L = 1$ means a linear relation, $R_L = 0$ indicates irreversibility and when $(0 < R_L < 1)$, the adsorption is favorable (Moridi and Gh 2022); K_F is the Freundlich constant, (mmol/g/(mmol/L)^{nF}; n_F is the Freundlich intensity parameter; b_S (L/mmol) and n_S are empirical constants of Sips model; q_{s1} and q_{s2} are the saturation adsorption capacity for the first and second layer respectively (mmol/g); k_1 and k_2 are the adsorption equilibrium constants, for the first and the second plateaus respectively and α and β are empirical parameters of Double Langmuir model.

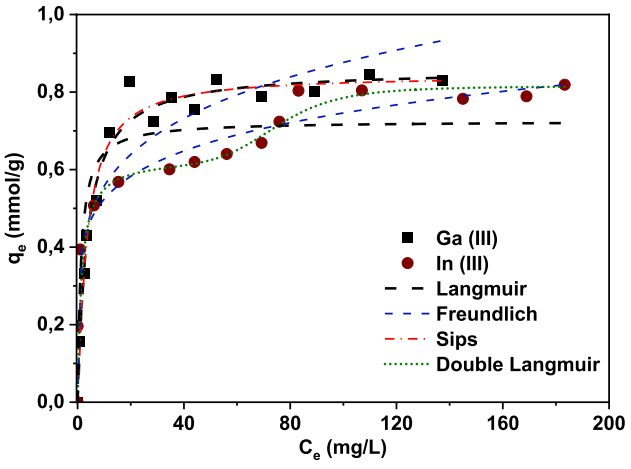

Fig. 9 Model fits to Ga^{3+} and In^{3+} isotherms at 298 K on H-CHA with sorbent doses of 1 g/L, free pH (< 3.0) and equilibrium time = 3 days

Table 6 Isotherm parameters calculated by non-linear regression

Isotherm model	Parameter	Metal	
		Ga^{3+}	In^{3+}
Langmuir	$q_{sat,exp}$ (mmol/g)	0.83	0.79
	q_{sat} (mmol/g)	0.86	0.73
	b_L (L/mg)	0.27	0.77
	R_L	1.8E-2	6.5E-3
	R^2	0.98	0.86
	RMSE (mmol/g)	2.10E-2	0.11
Freundlich	K_F (mmol/g)/(mmol/L)^{nF}	0.36	0.37
	N	5.09	6.51
	R^2	0.88	0.98
	RMSE (mmol/g)	0.12	1.6E-2
Sips	q_{sat} (mmol/g)	0.84	–
	K_s (L/mg)	0.28	–
	N	0.91	–
	R^2	0.98	–
	RMSE (mmol/g)	2.10E-2	–
Double Langmuir	q_{sat1} (mmol/g)	–	0.63
	q_{sat2} (mmol/g)	–	0.189
	K_1 (L/mg)	–	0.68
	α	–	$5.19 \cdot 10^{-13}$
	β	–	5.55
	R^2	–	0.93
	RMSE (mmol/g)	–	0.06

The experimental data, expressing the capacity as mmol/g, were fitted to the models (Fig. 9) by means of non-linear regression. The isotherm parameters obtained are shown in Table 6. The analysis of the fitting goodness was carried out considering the values of correlation coefficient (R^2) and root squared error (RMSE).

To describe the equilibrium sorption of Ga^{3+} onto H-CHA, the best model was Sips, because its high R^2 and low RMSE. Additionally, the value of q_{sat} obtained with this model is very close to the experimental one, suggesting that Sips equation can properly predict the adsorption system. As for the value of n, if the inverse is calculated, a value of 1.1 is obtained, which is close to 1, indicating that the adsorption isotherm exhibits a Langmuir-type behavior. In fact, if the Langmuir model results are observed, they are very similar to the estimated for Sips model, with a q_{sat} (0.86 mmol/g) only 3% higher than the experimental value (0.83 mmol/g). Moreover, this model describes the adsorption isotherm with only two parameters (q_{sat} and b_L), whereas the Sips model needs three parameters (q_{sat}, b_S and n_S). Regarding Freundlich model, in view of the R^2 (< 0.9) and RMSE values, the poor applicability of this model to the experimental data is demonstrated.

With regards to In^{3+} isotherm, Freundlich equation seems to be the model which best describe the adsorption of this

metal on H-CHA by obtaining a high R^2 value and a low RMSE. The inverse of parameter n of this model is 0.15. This very close to 0 value indicates the heterogeneity of the adsorbent surface as well as a favorable adsorption process. As for the Double Langmuir model, although the goodness of the fit is slightly lower than Freundlich's one, this model can define the multilayer of the adsorption isotherm as well as the saturation capacity for each of the plateaus. So, the model that best describes indium adsorption is Double Langmuir because it can predict the multilayer associated with the indium ion rearrangement, as previously discussed.

Regarding the favorability of the isotherms developed according to the Langmuir model, since for both models the value of R_L lies between 0 and 1, the adsorption is favorable at the selected temperature.

Competitive sorption kinetics

Sorption studies are usually performed on single solute systems. However, bimetallic sorption (Ga^{3+} and In^{3+}) should be studied to understand the competitive effect between the two metals and to study the effect of sorption time on the selective separation. Multimetallic studies try to approximate as much as possible to real cases, such as the one in which the two metals, Ga and In, are both present in leaching solutions from LED waste recovery treatment. After analyzing the adsorption isotherms of each metal ion separately, a series of competitive studies were carried out. These experiments were conducted at different concentration ratios: $[Ga^{3+}]=[In^{3+}]$ (0.5 mM for both metals); $[Ga^{3+}]=2\cdot[In^{3+}]$ (0.5 mM for Ga^{3+} and 0.25 mM for In^{3+}); and $[Ga^{3+}]=0.5\cdot[In^{3+}]$ (0.25 mM for Ga^{3+} and 0.5 mM for In^{3+}). The results obtained are displayed in Fig. 10. Figure 11 shows the variation of the q_{Ga3+}/q_{In3+} with the $[Ga^{3+}]/[In^{3+}]$ in the initial solution.

Regardless of the metal concentrations in the initial solution, q_{Ga3+} was greater than q_{In3+}. The comparison is made in Fig. 10. When the gallium concentration was higher than the indium concentration (Fig. 10(A)), H-CHA zeolite reached a q_{Ga3+}/q_{In3+} ratio of 2.9. This ratio decreased to 2.4 for the same concentration (Fig. 10(B)) and to 1.1 for higher indium concentration (Fig. 10(C)). The ion exchange capacity and selectivity for zeolites are mostly dependent on the exchangeable cations available, concentration of the solution, presence of other cations, and the properties of the zeolite: framework, Si/Al ratio, channel system, etc. (Baek et al. 2018). The selectivity to gallium was due to the charge of the predominant gallium species in solution at pH 3 (Fig. 8). The structure of the H-CHA zeolite, where the cationic sites are associated to the negative charge of the oxygen atoms of the structure, conditions the specific geometry of the cationic sites being easier the sorption of less charged cations ($Ga(OH)^{2+}$). When indium concentration in the solution was higher than the gallium concentration, the sorption

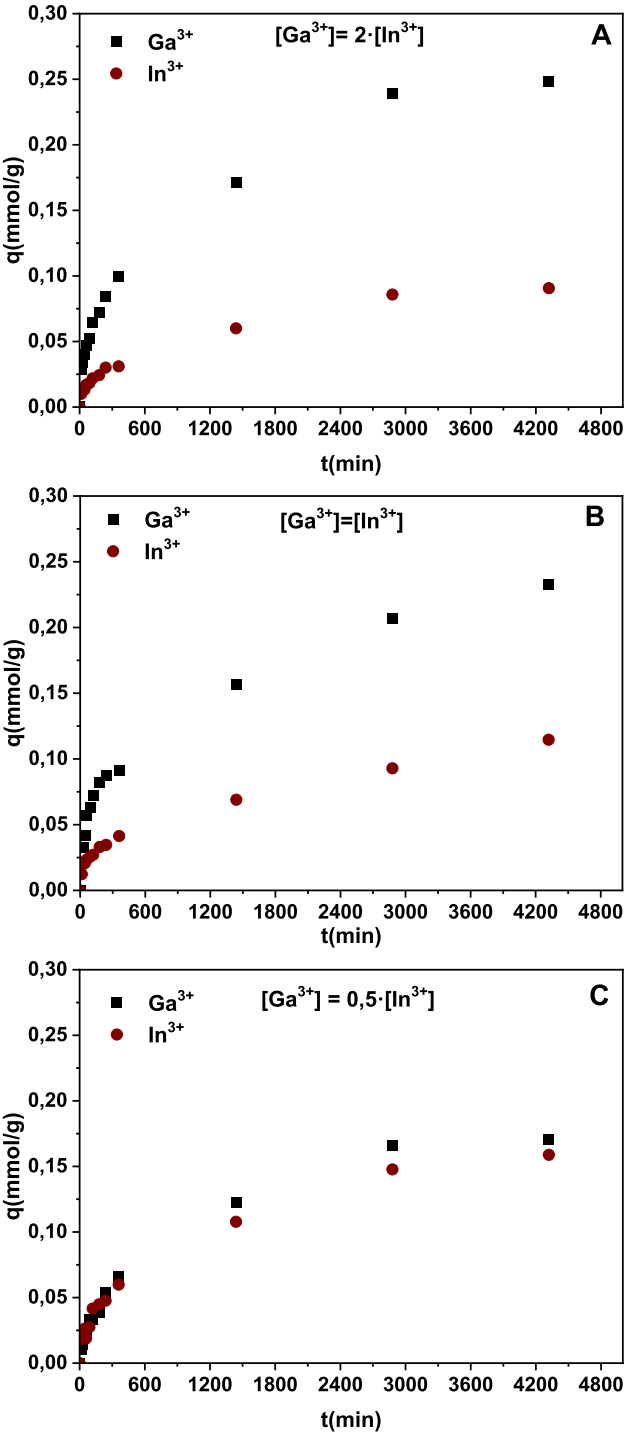

Fig. 10 Competitive adsorption kinetics of Ga^{3+} and In^{3+} on H-CHA at 298 K, doses: 1 g/L of H-CHA, free pH. (a) $[Ga^{3+}]=2\cdot[In^{3+}]$; (b) $[Ga^{3+}]=[In^{3+}]$; (c) $[Ga^{3+}]=0.5\ [In.^{3+}]$

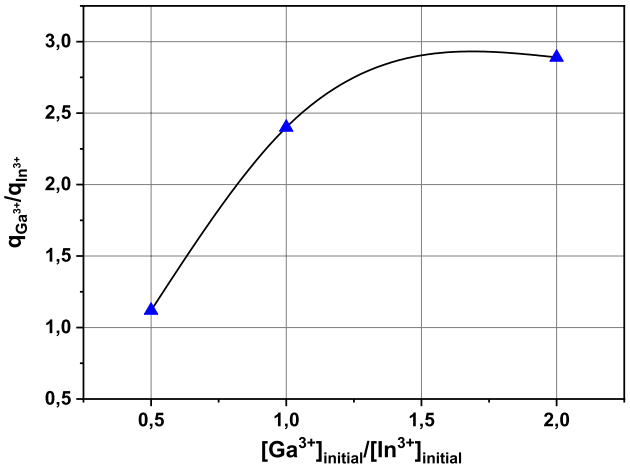

Fig. 11 Variation of the q_{Ga3+}/q_{In3+} vs. $[Ga^{3+}]_{initial}/[In^{3+}]_{initial}$

of gallium decreased to similar values as for In^{3+} due to the predominant effect of the higher concentration of In^{3+} in solution, the driving force toward In^{3+} sorption is greater.

The experimental sorption capacity values for each metal were compared with the theoretical values that would be achieved with a monometallic solution. The theoretical capacity values were obtained from the sorption isotherms (Fig. 7). Table 7 summarizes this comparison. In this table, theoretical values were expressed with "t" whereas the experimental ones with "exp". The values, expressed in percentage, in parentheses in Table 7 have been calculated as the experimental/theoretical ratio to see the difference from having one metal in the medium to both. Additionally, the ratio Ga^{3+} adsorbed between In^{3+} sorbed have been calculated.

Table 7 shows that the experimental sorption capacity values achieved were lower than those that would be obtained with Ga^{3+} and In^{3+} in monometallic solution. When the two metals are together in the solution, there is a competitive effect between both cations for the sorption sites, resulting in a decrease of both metal removal from the aqueous solution. However, the sum of both sorption capacities ($(q_{exp})_{Ga}{}^{3+} + (q_{exp})_{In}{}^{3+}$) reached the same value (≈ 0.34 mmol/g). This indicated that a maximum sorption capacity existing for both cations in solution regardless of the initial concentration ratio. A shielding effect occurred between the two cations, which prevented the theoretical sorption capacities from being reached. Since the concentration of gallium in LED leachates is higher than that of indium (Li et al. 2009), it will be possible to obtain a certain degree of selective separation toward gallium using H-CHA zeolite, retaining more gallium load since those cations are predominant with regard to indium ones. It is important to note that CHA is a natural zeolite that can be considered as a low-cost sorbent, and the modification to obtain the H-CHA zeolite was carried out using only one zeolite washing step. Further improvements in the protonation step could be made to increase the sorption capacity, while maintaining the buffering effect in the pH so that Ga^{3+} and In^{3+} would not precipitate during the process.

Conclusions

Chabazite, a low-cost zeolite, was able to remove gallium and indium ions from aqueous solutions. Protonation of the chabazite was necessary to avoid metal precipitation during the sorption process. This protonation was achieved under mild conditions, by one washing step with dilute HCl, which allowed the crystalline structure and the crystallinity degree to be maintained. The comparison made between the zeolites and the carbonaceous materials showed that the former presented a much higher sorption capacity, between 10 and 30 times higher, due to the cation exchange sites present in the chabazite (sites II, III, and IV). Chabazite was able to remove both metals with sorption capacities of 56 mg/g (0.83 mmol/g) and 92 mg/g (0.79 mmol/g)

Table 7 Comparison of theoretical (t) and experimental (exp) values of adsorption capacity and removal percentage

	$[Ga^{3+}] = 2 \cdot [In^{3+}]$		$[Ga^{3+}] = [In^{3+}]$		$[Ga^{3+}] = 0.5 \cdot [In^{3+}]$	
	Ga^{3+}	In^{3+}	Ga^{3+}	In^{3+}	Ga^{3+}	In^{3+}
q_t (mmol/g)	0.42	0.25	0.42	0.45	0.22	0.45
q_{exp} (mmol/g)*	0.25 (60%)	0.09 (36%)	0.23 (55%)	0.11 (24%)	0.17 (77%)	0.16 (36%)
$(q_{exp})_{Ga3+} + (q_{exp})_{In3+}$ (mmol/g)**	0.34 (80.7%)		0.35 (82.7%)		0.33 (73.2%)	
$Ga^{3+}{}_{sorbed}/In^{3+}{}_{sorbed}$ (%/%)	2.8		2.1		1.1	

* The values in parentheses indicate the percentage of the theoretical value, ** the value in brackets indicates the percentage of the maximum theoretical value with respect to the maximum adsorption capacity (gallium or indium)

for gallium and indium, respectively, with Ga^{3+} sorption being accurately described by Sips model and In^{3+} sorption by Freundlich model. The chabazite showed higher affinity for gallium than for indium when both metals were present in the solution, reaching a $Ga^{3+}{}_{sorbed}/In^{3+}{}_{sorbed}$ molar ratio almost 3 for $[Ga^{3+}]=2\cdot[In^{3+}]$, due to the behavior of both metals in aqueous solution at the sorption pH, $Ga(OH)^{2+}$ for gallium and In^{3+} for indium. The structure of the H-CHA zeolite conditioned the specific geometry of the cationic sites, being easier the sorption of less charged cations, as $Ga(OH)^{2+}$. Since the concentration of gallium in LED leachates is higher than that of indium, it is possible to achieve a certain degree of selective separation toward gallium using H-CHA zeolite. Sorption with protonated chabazite can be used in the treatment of light-emitting diodes (LEDs) leachates used for the dual purpose of water purification and selective separation of metals.

Author contribution Patricia Sáez: conceptualization, investigation, data curation, original draft. Eduardo Díez: conceptualization, supervision, data curation, original draft, review and editing. José María Gómez: conceptualization, funding acquisition, project administration, resources, data curation, supervision, original draft, review and editing. Carmen López: investigation, data curation. Araceli Rodríguez: conceptualization, funding acquisition, project administration, resources, supervision, review and editing. Naby Conte: conceptualization, investigation, data curation, original draft, review and editing. Mercedes Lobete: investigation, data curation.

Funding The authors gratefully acknowledge the financial support from Ministerio de Economía y Competitividad CTQ2014-59011-R (REMEWATER) and from Ministerio de Ciencia e Innovación PID2021-125797OB-I00 (BIORe_WASTES). PSG was supported by a FPU contract-fellowship (Formación de Profesorado Universitario) from Ministerio de Educación Cultura y Deporte (FPU 14/00500). Special acknowledgement to St. Cloud mining for supplying the chabazite used in this research, Cherry Below Brewery, S.L. for supplying the beer bagasse, the Correlation Spectroscopy Research Centre, and the X-Ray Diffraction Unit of the Complutense University of Madrid for both helping with the characterization.

Data availability The data will be available on request.

Declarations

Consent to participate Informed consent was obtained from all individual participants included in the study.

Consent for publication The participants have consented to the submission of the manuscript to the journal.

Competing interests The authors declare no competing interests.

References

Abdelwahab O, Thabet WM (2023) Natural zeolites and zeolite composites for heavy metal removal from contaminated water and their applications in aquaculture Systems: A review. Egypt J Aquat Res 49:431–443. https://doi.org/10.1016/j.ejar.2023.11.004

Ahirwar R, Tripathi AK (2021) E-waste management: a review of recycling process, environmental and occupational health hazards, and potential solutions. Environ Nanotechnol Monit Manag 15:100409. https://doi.org/10.1016/j.enmm.2020.100409

Akcil A, Agcasulu I, Swain B (2019) Valorization of waste LCD and recovery of critical raw material for circular economy: a review. Resour Conserv Recycl 149:622–637. https://doi.org/10.1016/j.resconrec.2019.06.031

Alguacil FJ, Lopez FA, Rodriguez O et al (2016) Sorption of indium (III) onto carbon nanotubes. Ecotoxicol Environ Saf 130:81–86. https://doi.org/10.1016/j.ecoenv.2016.04.008

Anukam AI, Mamphweli SN, Reddy P, Okoh OO (2016) Characterization and the effect of lignocellulosic biomass value addition on gasification efficiency. Energy Explor Exploit 34:865–880. https://doi.org/10.1177/0144598716665010

Aysan H, Edebali S, Ozdemir C et al (2016) Use of chabazite, a naturally abundant zeolite, for the investigation of the adsorption kinetics and mechanism of methylene blue dye. Microporous Mesoporous Mater 235:78–86. https://doi.org/10.1016/j.micromeso.2016.08.007

Baek W, Ha S, Hong S et al (2018) Cation exchange of cesium and cation selectivity of natural zeolites: Chabazite, stilbite, and heulandite. Microporous Mesoporous Mater 264:159–166. https://doi.org/10.1016/j.micromeso.2018.01.025

Baerlocher C, McCusker LB, Olson DH (2007) CHA - R3¯m. In: Baerlocher C, McCusker LB, Olson DH (eds) Atlas of zeolite framework types, 6th edn. Elsevier Science B.V, Amsterdam, pp 96–97

Baldé CP, Kuehr R, Yamamoto T, McDonald R, D'Angelo E, Althaf S, Bel G, Deubzer O, Fernandez-Cubillo E, Forti V, Gray V, Hera S, Honda S, Iattoni G, Khetriwal DS, di Cortemiglia VL, Lobuntsova Y, Nnorom I, Pralat N, Wagner M (2024) International telecommunication union (ITU) and United Nations institute for training and research (UNITAR). Global E-waste Monitor 2024, Geneva/Bonn

Balinski A, Recksiek V, Stoll M et al (2022) Liberation and separation of valuable components from LED modules: presentation of two innovative approaches. Recycling 7:26. https://doi.org/10.3390/recycling7030026

Breck DW (1973) Zeolite molecular sieves: structure, chemistry, and use. Wiley

Cenci MP, Dal Berto FC, Schneider EL, Veit HM (2020) Assessment of LED lamps components and materials for a recycling perspective. Waste Manag 107:285–293. https://doi.org/10.1016/j.wasman.2020.04.028

Chen WS, Chung YF, Tien KW (2020) Recovery of gallium and indium from waste light emitting diodes. In: Proceedings of the 15th international symposium on East Asian resources recycling technology, EARTH 2019, vol 29, Pyeongchang, pp 81– 88

Chen W-S, Hsu L-L, Wang L-P (2018) Recycling the GaN waste from LED industry by pressurized leaching method. Metals 8:861. https://doi.org/10.3390/met8100861

Conte N, Gómez JM, Díez E et al (2022) Sequential separation of cobalt and lithium by sorption: Sorbent set selection. Sep Purif Technol 303:122199. https://doi.org/10.1016/j.seppur.2022.122199

de Oliveira RP, Benvenuti J, Espinosa DCR (2021) A review of the current progress in recycling technologies for gallium and rare earth elements from light-emitting diodes. Renew Sustain Energy Rev 145:111090. https://doi.org/10.1016/j.rser.2021.111090

Denayer JFM, Devriese LI, Couck S et al (2008) Cage and window effects in the adsorption of n-alkanes on chabazite and SAPO-34. J Phys Chem C 112:16593–16599. https://doi.org/10.1021/jp804349v

Díez E, Gómez JM, Rodríguez A et al (2020) A new mesoporous activated carbon as potential adsorbent for effective indium

removal from aqueous solutions. Microporous Mesoporous Mater 295:109984. https://doi.org/10.1016/j.micromeso.2019.109984
Directorate-General for Internal Market I, Bobba S, Carrara S et al (2020) Critical raw materials for strategic technologies and sectors in the EU: a foresight study. Publications Office of the European Union, LU
Drzazga M, Palmowski A, Benke G et al (2021) Recovery of germanium and indium from leaching solution of germanium dross using solvent extraction with TOA, TBP and D2EHPA. Hydrometallurgy 202. https://doi.org/10.1016/j.hydromet.2021.105605
Egashira R, Tanabe S, Habaki H (2012) Adsorption of heavy metals in mine wastewater by Mongolian natural zeolite. Procedia Eng 42:49–57. https://doi.org/10.1016/j.proeng.2012.07.394
El Ouardi Y, Virolainen S, Salomon E et al (2023) The recent progress of ion exchange for the separation of rare earths from secondary resources—a review. Hydrometallurgy 218:106047. https://doi.org/10.1016/j.hydromet.2023.106047
European Commission. Directorate General for Internal Market, Industry,Entrepreneurship and SMEs (2023) European commission, critical materials for strategic technologies and sectors in the EU - a foresight study, 2020. European commission, study on the critical raw materials for the EU 2023 – Final Report
Foster MD, Rivin I, Treacy MMJ, Delgado Friedrichs O (2006) A geometric solution to the largest-free-sphere problem in zeolite frameworks. Microporous Mesoporous Mater 90:32–38. https://doi.org/10.1016/j.micromeso.2005.08.025
Freundlich HMF (1906) Over the adsorption in solution. J Phys Chem 57:385–471
Galán J, Rodríguez A, Gómez JM et al (2013) Reactive dye adsorption onto a novel mesoporous carbon. Chem Eng J 219:62–68. https://doi.org/10.1016/j.cej.2012.12.073
Gallant J, Prakash A, Hogg LVEW (2009) Removal of selected radionuclides and metal contaminants by natural zeolites from liquid effluents. In: Curran Associates Inc (ed) 30th Annual Canadian Nuclear Society Conference and 33rd CNS/CNA Student Conference 2009. Canadian Nuclear Society, Calgary, pp 599–610
Giles CH, MacEwan TH, Nakhwa SN, Smith D (1960) Studies in adsorption. Part XI. A system of classification of solution adsorption isotherms, and its use in diagnosis of adsorption mechanisms and in measurement of specific surface areas of solids. J Chem Soc (Resumed) 846:3973–3993. https://doi.org/10.1039/jr9600003973
Girtan M, Wittenberg A, Grilli ML et al (2021) The critical raw materials issue between scarcity, supply risk, and unique properties. Materials (Basel) 14:1826. https://doi.org/10.3390/ma14081826
Göltl F, Hafner J (2011) Alkane adsorption in Na-exchanged chabazite: the influence of dispersion forces. J Chem Phys 134. https://doi.org/10.1063/1.3549815
Gómez JM, Romero MD, Fernández TM, Díez E (2012) Immobilization of β-glucosidase in fixed bed reactor and evaluation of the enzymatic activity. Bioprocess Biosyst Eng 35:1399–1405. https://doi.org/10.1007/s00449-012-0728-y
González-Crisostomo JC, López-Juárez R, Yocupicio-Gaxiola RI et al (2022) chabazite synthesis and its exchange with Ti, Zn, Cu, Ag and Au for efficient photocatalytic degradation of methylene blue dye. Int J Mol Sci 23:1730. https://doi.org/10.3390/ijms23031730
Grevtsov N, Chubenko E, Bondarenko V et al (2021) Electrochemical deposition of indium into oxidized and unoxidized porous silicon. Thin Solid Films 734:138860. https://doi.org/10.1016/j.tsf.2021.138860
Haan AB de (2015) Adsorption and ion exchange. Process technology: an introduction, Berlin, München. De Gruyter, Boston, pp 177–196. https://doi.org/10.1515/9783110336726-010
Hall KR, Eagleton LC, Acrivos A, Vermeulen T (1966) Pore- and solid-diffusion kinetics in fixed-bed adsorption under constant-pattern conditions. Ind Eng Chem Fund 5:212–223. https://doi.org/10.1021/i160018a011
Hinz C (2001) Description of sorption data with isotherm equations. Geoderma 99:225–243. https://doi.org/10.1016/S0016-7061(00)00071-9
Ibrahim KM, Khoury HN, Tuffaha R (2016) Mo and Ni removal from drinking water using zeolitic tuff from Jordan. Minerals 6:116. https://doi.org/10.3390/min6040116
Jeon C, Cha J-H, Choi J-Y (2015) Adsorption and recovery characteristics of phosphorylated sawdust bead for indium(III) in industrial wastewater. J Ind Eng Chem 27:201–206. https://doi.org/10.1016/j.jiec.2014.12.036
Kennedy DA, Tezel FH (2018) Cation exchange modification of clinoptilolite—Screening analysis for potential equilibrium and kinetic adsorption separations involving methane, nitrogen, and carbon dioxide. Microporous Mesoporous Mater 262:235–250. https://doi.org/10.1016/j.micromeso.2017.11.054
Khezerloo S, Nasirpour N, Pourhossein F, Mousavi SM (2023) Bioleaching of indium from spent light-emitting diode monitors and selective recovery followed by solvent extraction. J Environ Manage 335:117520. https://doi.org/10.1016/j.jenvman.2023.117520
Kim M-S, Kim J-G (2020) Adsorption characteristics of spent coffee grounds as an alternative adsorbent for cadmium in solution. Environments 7:24. https://doi.org/10.3390/environments7040024
Korkuna O, Leboda R, Skubiszewska-Zie,ba J et al (2006) Structural and physicochemical properties of natural zeolites: clinoptilolite and mordenite. Microporous Mesoporous Mater 87:243–254. https://doi.org/10.1016/j.micromeso.2005.08.002
Kuehr R (2024) Global E-waste monitor 2024: electronic waste rising five times faster than documented E-waste recycling. United Nations Institute for Training and Research, Geneva
Lahti J, Vazquez S, Virolainen S et al (2020) Membrane filtration enhanced hydrometallurgical recovery process of indium from waste LCD panels. J Sustain Metall 6:576–588. https://doi.org/10.1007/s40831-020-00293-4
Langmuir I (1917) The constitution and fundamental properties of solids and liquids. II. LIQUIDS. 1. J Am Chem Soc 39:1848–1906. https://doi.org/10.1021/ja02254a006
Lee S-K, Lee U-H (2016) Adsorption and desorption property of iminodiacetate resin (Lewatit® TP207) for indium recovery. J Ind Eng Chem 40:23–25. https://doi.org/10.1016/j.jiec.2016.05.016
Li Y, Xi M, Kong F, Yu C (2009) Experimental study on the removal of arsenic in waste water from semiconductor manufacturing. J Water Resour Prot 1:48–51. https://doi.org/10.1109/ICBBE.2008.1025
Liu JS, Chen H, Chen XY et al (2006) Extraction and separation of In(III), Ga(III) and Zn(II) from sulfate solution using extraction resin. Hydrometallurgy 82:137–143. https://doi.org/10.1016/j.hydromet.2006.03.008
Lu F, Xiao T, Lin J et al (2017) Resources and extraction of gallium: a review. Hydrometallurgy 174:105–115. https://doi.org/10.1016/j.hydromet.2017.10.010
Martins TR, Tanabe EH, Bertuol DA (2020) Innovative method for the recycling of end-of-life LED bulbs by mechanical processing. Resour Conserv Recycl 161:104875. https://doi.org/10.1016/j.resconrec.2020.104875
Meng J, He C, Li Y et al (2021) Enhanced adsorption and separation of gallium using silica-based P507-TBP/SiO2–P adsorbent from sulfuric acid solution. Microporous Mesoporous Mater 314:110859. https://doi.org/10.1016/j.micromeso.2020.110859
Michaels KC (2021) The role of critical minerals in clean energy transitions. IEA (International Energy Agency) Report, p 7
Mir S, Vaishampayan A, Dhawan N (2022) A review on recycling of end-of-life light-emitting diodes for metal recovery. JOM 74:599–611. https://doi.org/10.1007/s11837-021-05043-9

Moridi H, Gh AB (2022) Sodium alginate/polyvinyl pyrrolidone/zinc oxide @silica Schiff-base nanofiber membrane for single and binary removal of copper and nickel cations from aqueous medium. Res Chem Intermed 48:4643–4670. https://doi.org/10.1007/s11164-022-04834-2

Mozgawa W, Król M, Barczyk K (2011) FT-IR studies of zeolites from different structural groups. Chemik 65:667–674

Mumpton FA, Ormsby WC (1976) Morphology of zeolites in sedimentary rocks by scanning electron microscopy. Clays Clay Miner 24:1–23. https://doi.org/10.1346/CCMN.1976.0240101

Nikulski JS, Ritthoff M, von Gries N (2021) The potential and limitations of critical raw material recycling: the case of LED lamps. Resources 10:37. https://doi.org/10.3390/resources10040037

Pennesi C, Amato A, Occhialini S et al (2019) Adsorption of indium by waste biomass of brown alga Ascophyllum nodosum. Sci Rep 9:16763. https://doi.org/10.1038/s41598-019-53172-8

Phadke NM, Van der Mynsbrugge J, Mansoor E et al (2018) Characterization of isolated Ga3+ cations in Ga/H-MFI prepared by vapor-phase exchange of H-MFI zeolite with GaCl3. ACS Catal 8:6106–6126. https://doi.org/10.1021/acscatal.8b01254

Pham TD, Hudson MR, Brown CM, Lobo RF (2014) Molecular basis for the high CO2 adsorption capacity of chabazite zeolites. Chemsuschem 7:3031–3038. https://doi.org/10.1002/cssc.201402555

Pinedo-Torres LA, Bonilla-Petriciolet A, García-Arreola ME et al (2023) Adsorption of arsenic, lead, cadmium, and chromium ions from aqueous solution using a protonated chabazite: preparation, characterization, and removal mechanism. Adsorpt Sci Technol 2023:2018121. https://doi.org/10.1155/2023/2018121

Qasem NAA, Mohammed RH, Lawal DU (2021) Removal of heavy metal ions from wastewater: a comprehensive and critical review. npj Clean Water 4:1–15. https://doi.org/10.1038/s41545-021-00127-0

Qi H, Gong N, Zhang S-Q et al (2023) Research progress on the enrichment of gallium in bauxite. Ore Geol Rev 160:105609. https://doi.org/10.1016/j.oregeorev.2023.105609

Qin J, Ning S, Xu J et al (2023) Separation and recovery of indium in hazardous liquid crystal display treatment by a novel silica adsorbent: study on adsorption mechanism and process design. J Clean Prod 425:138999. https://doi.org/10.1016/j.jclepro.2023.138999

Rahimifard S, Trollman H (2018) UN sustainable development goals: an engineering perspective. Int J Sustain Eng 11:1–3. https://doi.org/10.1080/19397038.2018.1434985

Rautela R, Arya S, Vishwakarma S et al (2021) E-waste management and its effects on the environment and human health. Sci Total Environ 773:145623. https://doi.org/10.1016/j.scitotenv.2021.145623

Richter JL, Van Buskirk R, Dalhammar C, Bennich P (2019) Optimal durability in least life cycle cost methods: the case of LED lamps. Energ Effi 12:107–121. https://doi.org/10.1007/s12053-018-9662-4

Rivera-Ramos ME, Hernández-Maldonado AJ (2007) Adsorption of N2 and CH4 by ion-exchanged silicoaluminophosphate nanoporous sorbents: interaction with monovalent, divalent, and trivalent cations. Ind Eng Chem Res 46:4991–5002. https://doi.org/10.1021/ie061016m

Roosen J, Mullens S, Binnemans K (2017) Chemical immobilization of 8-hydroxyquinoline and 8-hydroxyquinaldine on chitosan-silica adsorbent materials for the selective recovery of gallium from Bayer liquor. Hydrometallurgy 171:275–284. https://doi.org/10.1016/j.hydromet.2017.05.026

Reuters (2023) Beijing's curbs on niche metal exports threaten China supply glut. In: Reuters. https://www.reuters.com/markets/commodities/beijings-curbs-niche-metal-exports-threaten-china-supply-glut-2023-07-06/. Accessed 24 May 2024

Sáez P, Bernabé I, Gómez JM et al (2023) Assessment of two materials as adsorbents for the effective removal and further pre-concentration of gallium from aqueous solutions: mesoporous carbon vs. clinoptilolite. Separations 10:349. https://doi.org/10.3390/separations10060349

Sáez P, Rodríguez A, Gómez JM et al (2021) H-Clinoptilolite as an efficient and low-cost adsorbent for batch and continuous gallium removal from aqueous solutions. J Sustain Metal. https://doi.org/10.1007/s40831-021-00437-0

Saikia S, Sinharoy A, Lens PNL (2022) Adsorptive removal of gallium from aqueous solution onto biogenic elemental tellurium nanoparticles. Sep Purif Technol 286:120462. https://doi.org/10.1016/j.seppur.2022.120462

Saravanan A, Senthil Kumar P, Jeevanantham S et al (2021) Effective water/wastewater treatment methodologies for toxic pollutants removal: Processes and applications towards sustainable development. Chemosphere 280:130595. https://doi.org/10.1016/j.chemosphere.2021.130595

Segala BN, Wenzel BM, Power NP et al (2023) Efficient gallium recovery from aqueous solutions using polyacrylonitrile nanofibers loaded with D2EHPA. Metals 13:1545. https://doi.org/10.3390/met13091545

Shang J, Hanif A, Li G et al (2020) Separation of CO2 and CH4 by pressure swing adsorption using a molecular trapdoor chabazite adsorbent for natural gas purification. Ind Eng Chem Res 59:7857–7865. https://doi.org/10.1021/acs.iecr.0c00317

Shrestha R, Ban S, Devkota S et al (2021) Technological trends in heavy metals removal from industrial wastewater: a review. J Environ Chem Eng 9:105688. https://doi.org/10.1016/j.jece.2021.105688

Singh RK, Webley P (2005) Adsorption of N2, O2, and Ar in potassium chabazite. Adsorption 11:173–177. https://doi.org/10.1007/s10450-005-5918-3

Sips R (1950) On the structure of a catalyst surface. II. J Chem Phys 18:1024–1026. https://doi.org/10.1063/1.1747848

Solisio C, Aliakbarian B (2017) Methylene blue adsorption using chabazite: kinetics and equilibrium modelling. Can J Chem Eng 95:1760–1767. https://doi.org/10.1002/cjce.22838

Song SJ, Le MN, Lee MS (2020) Separation of Gallium(III) and Indium(III) by solvent extraction with ionic liquids from hydrochloric acid solution. Processes 8:1347. https://doi.org/10.3390/pr8111347

Ujaczki É, Courtney R, Cusack P et al (2019) Recovery of Gallium from bauxite residue using combined oxalic acid leaching with adsorption onto zeolite HY. J Sustain Metall 5:262–274. https://doi.org/10.1007/s40831-019-00226-w

Watson GC, Jensen NK, Ru TE et al (2012) Volumetric adsorption measurements of N2 , CO2 , CH4 , and a CO2 + CH4 mixture on a natural chabazite from (5 to 3000 869 kPa). J Chem Eng Data 57:93–101

Worch E (2012) Adsorption technology in water treatment: fundamentals, processes, and modeling. De Gruyter, Boston. https://doi.org/10.1515/9783110240238

Yakout SM, Borai EH (2014) Adsorption behavior of cadmium onto natural chabazite: Batch and column investigations. Desalin Water Treat 52:4212–4222. https://doi.org/10.1080/19443994.2013.803938

Yue Q, Halamek J, Rainer DN et al (2022) Tuning the CHA framework composition by isomorphous substitution for CO2/CH4 separation. Chem Eng J 429:131277. https://doi.org/10.1016/j.cej.2021.131277

Rebello RZ, Lima MT, Yamane LH, Siman RR (2020) Characterization of end-of-life LED lamps for the recovery of precious metals and rare earth elements. Resour Conserv Recycl 153:104557. https://doi.org/10.1016/j.resconrec.2019.104557

Zeng W, Xu L, Wang Q et al (2022) Adsorption of Indium(III) ions from an acidic solution by using UiO-66. Metals 12:579. https://doi.org/10.3390/met12040579

Zhang J, Singh R, Webley PA (2008) Alkali and alkaline-earth cation exchanged chabazite zeolites for adsorption based CO2 capture. Microporous Mesoporous Mater 111:478–487. https://doi.org/10.1016/j.micromeso.2007.08.022

Zhang L, Wang Y, Guo X et al (2009) Separation and preconcentration of trace indium(III) from environmental samples with nanometer-size titanium dioxide. Hydrometallurgy 95:92–95. https://doi.org/10.1016/j.hydromet.2008.05.001

Zhao F, Zou Y, Lv X et al (2015) Synthesis of CoFe2O4–zeolite materials and application to the adsorption of gallium and indium. J Chem Eng Data 60:1338–1344. https://doi.org/10.1021/je501039u

Zhao Z, Li X, Chai Y et al (2016) Adsorption performances and mechanisms of Amidoxime resin toward Gallium(III) and Vanadium(V) from Bayer liquor. ACS Sustainable Chem Eng 4:53–59. https://doi.org/10.1021/acssuschemeng.5b00307

Zhao Z, Yang Y, Xiao Y, Fan Y (2012) Recovery of gallium from Bayer liquor: a review. Hydrometallurgy 125–126:115–124. https://doi.org/10.1016/j.hydromet.2012.06.002

Zheng K, Benedetti MF, Jain R et al (2024) Recovery of gallium (and indium) from spent LEDs: Strong acids leaching versus selective leaching by siderophore desferrioxamine E. Sep Purif Technol 338:126566. https://doi.org/10.1016/j.seppur.2024.126566